

Correlation of static speckle with sample properties in optical coherence tomography

Timothy R. Hillman, Steven G. Adie, Volker Seemann, and Julian J. Armstrong

*Optical+Biomedical Engineering Laboratory, School of Electrical, Electronic and Computer Engineering,
The University of Western Australia, Western Australia 6009, Australia*

Steven L. Jacques

Oregon Health and Science University, Portland, Oregon 97225-6622

David D. Sampson

*Optical+Biomedical Engineering Laboratory, School of Electrical, Electronic and Computer Engineering,
The University of Western Australia, Western Australia 6009, Australia*

Received August 2, 2005; revised October 7, 2005; accepted October 11, 2005

We present theoretical calculations, based on a random phasor sum model, which show that the optical coherence tomography speckle contrast ratio is dependent on the local density of scattering particles in a sample, provided that the effective number of scatterers in the probed volume is less than about five. We confirm these theoretical predictions experimentally, using suspensions of microspheres in water. The observed contrast ratios vary in value from the Rayleigh limit of 0.52 to in excess of 2, suggesting that the contrast ratio could be useful in optical coherence tomography, particularly when imaging in ultrahigh-resolution regimes. © 2006 Optical Society of America
OCIS codes: 030.6140, 170.4500, 290.5850.

In scattering media, optical coherence tomography¹ (OCT) signals are formed by the coherent addition of multiple backscattered optical fields. This gives rise to the speckle phenomenon,² the characteristic granular, or mottled, image appearance common to all coherent imaging modalities.³ OCT speckle is generally perceived to be a corrupting influence, limiting the ability of the technique to resolve sample structure. However, it can also be regarded as the carrier of sample information; indeed, the missing frequency characterization of speckle^{2,4} interprets the phenomenon as arising from the bandpass-filtering property of the OCT point-spread function. That is, the speckle is inherent to the narrow range of sample spatial frequencies that can be detected with OCT.

OCT speckle is known to be affected by the sample structure and motion of the scatterers within it, as well as by the spatial extent and temporal coherence of the light source, multiple scattering and phase aberrations of the propagating beam, and the aperture of the detector.² Most research on OCT speckle in static samples has involved attempts to mitigate its deleterious effects on image presentation. This has been achieved with some success via spatial, frequency, or angular compounding and various methods of image postprocessing.^{2,5,6} A less common perspective in OCT has been the exploitation of speckle as a source of useful information, although it is well known to be so in other areas of optical metrology.³ Temporally dynamic OCT speckle has been used to determine spatially resolved diffusion⁷ and flow⁸ in liquids, including human blood *in vivo*.⁹ With regard to static speckle, a study has been undertaken to distinguish tissue types by performing texture analysis on OCT images.¹⁰ In this Letter we demonstrate, theoretically and experimentally, a correlation be-

tween OCT speckle statistics and the sample's constitution and optical properties by means of the contrast ratio, the ratio of the OCT envelope signal's standard deviation to its mean. We consider only fully developed speckle, that is, speckle patterns that have not been subjected to any form of incoherent averaging. Our theoretical model is based on the sum of random phasors,¹¹ which has previously been successfully applied to the case of OCT.^{5,6} We show that when the OCT signal is derived from a large number of scatterers, there is negligible variation in the contrast ratio, but that it varies strongly when the effective number of scatterers is less than about five. We confirm theoretical predictions with experiments on suspensions of microspheres.

A turbid biological medium is most accurately represented as a spatially varying refractive index continuum.¹² Light scattering strength and directionality depend on the gradient of the refractive index. For simplicity, however, we adopt a particle model of tissue in which scatterers are randomly distributed throughout a sample. We assume that the speckle arises from the superposition of multiple waves that have been singly scattered from within the sample probe volume. We thereby neglect the effect of the wavefront distortion that occurs in propagating to and from the sample volume and the effect of any detected light that has undergone multiple scattering events.

The statistics of static OCT speckle have been previously described,^{2,5,6} based on a random phasor sum and the validity of the central limit theorem, and experimentally verified for large numbers of scatterers. The envelope of the OCT interferogram may be expressed as $I_{\text{env}} = 2\sqrt{I_R} \left| \sum_{i=1}^n E_{Si} \right|$, where I_R is the detected reference intensity, n is the number of scat-

tered sample waves contributing to the signal, and $E_{S_i} = A_i \exp(j\theta_i)$ is the complex phasor representation of the detected field from the i th wave, with positive amplitude A_i and phase θ_i . We seek to determine the statistics of the random phasor sum envelope $|\sum_{i=1}^n E_{S_i}|$, based on the joint distributions of the amplitudes and phases of E_{S_i} and n . We assume that the particles are distributed uniformly throughout the sample, and that each backscatters equally, unaffected by any of the other particles. Therefore, the various E_{S_i} are independent, and the value of each E_{S_i} depends only on the location of the i th particle, (x_i, y_i, z_i) . Its phase is determined by its axial optical distance (modulo $\bar{\lambda}/2$, where $\bar{\lambda}$ is the mean wavelength), and its amplitude by its position in the sample volume [with dimensions determined by the coherence length of the source, ℓ_c , and the lateral ($1/e^2$ intensity) diameter of the focused beam, D]. If $\bar{\lambda}/2 \ll \ell_c$, then the phase of the i th phasor can be considered independent of its amplitude and uniformly distributed on $[0, 2\pi)$. To determine the distribution (pdf) of the amplitude A_i , we introduce the confocal gate function $h(x, y, z)$, which gives the detected (intensity) response to a scatterer at location (x, y, z) , and the coherence gate function $\gamma(z)$, the real envelope of the complex degree of coherence.⁵ The amplitude is given by⁵ $A_i = f(x_i, y_i, z_i) = \sqrt{h(x_i, y_i, z_i)}\gamma(z_i)$, and the function f is normalized so that its maximum value is 1. If we assume that the confocal and coherence gates are aligned (at $z=0$), we may approximate it by a three-dimensional Gaussian, given by

$$f(x, y, z) = \exp\left\{-\left[\frac{x^2 + y^2}{(D/2)^2} + \frac{2\pi z^2}{L^2}\right]\right\}, \quad (1)$$

where $L = \ell_c/n_g$, and n_g is the group refractive index of the medium. For a given $r_0 \in (0, 1)$, let $V(r_0)$ be the volume of the region for which $f(x, y, z) > r_0$. If r_0 is chosen to be sufficiently small, then the effect of scatterers from outside this region on the detected signal is negligible. Therefore, considering only scatterers within the region, the pdf of their phasor amplitudes is

$$g(r; r_0) = \begin{cases} -[3/(2r \ln r_0)](\ln r/\ln r_0)^{1/2} & \text{if } r \in (r_0, 1) \\ 0 & \text{otherwise} \end{cases}. \quad (2)$$

The number of scatterers in the region of volume $V(r_0)$, n , is a random variable that is independent of the values of E_{S_i} and may be assumed to be Poisson distributed with mean parameter $NV(r_0)$, where N is the volume density of particles.

Given these assumptions, we determine the contrast ratio of the detected signal. Numerous methods for calculating the pdf of the envelope of the sum of random phasors exist.¹³ For a given n , expressions for the first and second moments of the random phasor sum, $\mu_n^{(1)}$ and $\mu_n^{(2)}$, can be determined by using one

such method. Forming weighted averages over all n according to the Poisson distribution yields the contrast ratio

$$\text{CR} = [\overline{\mu_n^{(2)}} - \overline{\mu_n^{(1)}}^2]^{1/2}/\overline{\mu_n^{(1)}}, \quad (3)$$

where $\overline{\mu_n^{(h)}} = \sum_{n=0}^{\infty} \text{Poi}[n; NV(r_0)]\mu_n^{(h)}$ and $\text{Poi}(n; \sigma) = \sigma^n \exp(-\sigma)/n!$. For very small values of $NV(r_0)$, only the terms corresponding to $n=1$ contribute significantly to Eq. (3) (since $\mu_0^{(1)} = \mu_0^{(2)} = 0$). In this region, $\text{CR} \propto 1/\sqrt{N}$, increasing without bound as $N \rightarrow 0$. For large values of N , CR approaches its Rayleigh-limited value (determined by the central limit theorem¹¹) of $\sqrt{4/\pi-1} = 0.52$. For a fixed concentration N , as the volume of interest $V(r_0)$ increases without bound (i.e., as $r_0 \rightarrow 0^+$), CR converges to values dependent only on D^2LN . We define this quantity to be the effective number of scatterers (ENS) contributing to the OCT signal, and hereafter define CR to be its value in the limit. Under our model, CR is a strictly decreasing function of ENS, and it exceeds 0.58 when ENS=5, a quantity over 10% greater than its value in the Rayleigh limit.

We performed experimental contrast-ratio measurements on sample suspensions of polystyrene microspheres in water ($n_g = 1.34$). Figure 1 shows the OCT system schematic. Light from a broadband source ($\bar{\lambda} = 1330$ nm; spectral bandwidth $\Delta\lambda = 45$ nm) is directed into both a reference and a sample arm via a 50/50 coupler. Reference arm axial scanning is performed with a frequency-domain optical delay line⁵ (FD-ODL), and sample arm lateral scanning with a galvanometer mirror and objective lens setup (NA=0.19). The photoreceiver signal is input into a low-noise bandpass filter–preamplifier before A/D conversion. The digitized full-fringe signal was processed by first applying a bandpass filter (passband 40–60 kHz), and calculating the signal envelope. The measured values of system sensitivity, D , and L were 118 dB, 4.5 μm , and 20 μm , respectively.

The microsphere sample concentrations ranged from 5.8×10^{10} to 2.8×10^8 particles/ml, obtained by performing successive dilutions of the stock solution. A droplet of each suspension was placed on a glass window, and the sample beam was focused into it from beneath. 71 frames, each comprising 64 axial scans, were recorded at 0.8 frames/s. Brownian motion of the particles, together with lateral scanning over 120 μm , ensured that a large ensemble of speckle states were probed, enabling accurate mea-

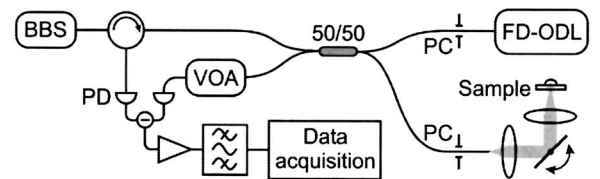


Fig. 1. Schematic of OCT system. BBS, broadband source; PC, polarization controller; FD-ODL, frequency-domain optical delay line; VOA, variable optical attenuator; PD, photodetector.

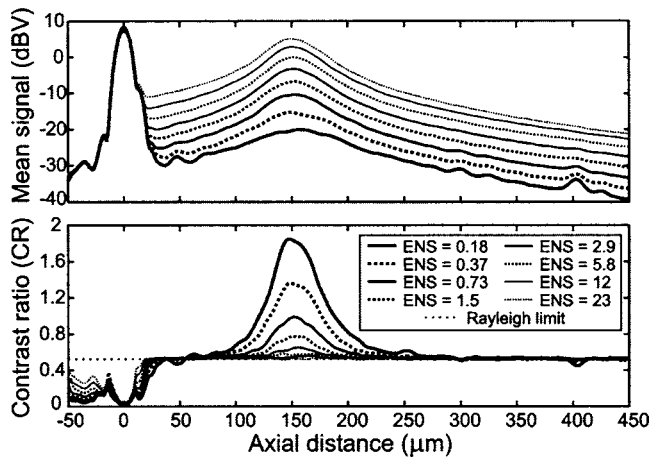


Fig. 2. Plot of mean detected signal (upper) and contrast ratio (lower) versus axial position (referenced to the sample-glass interface), for $0.51 \mu\text{m}$ microspheres.

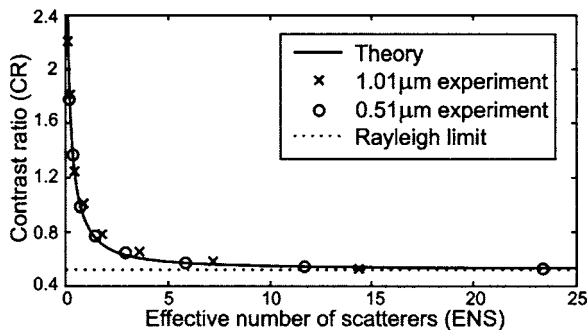


Fig. 3. Plot of contrast ratio versus effective number of scatterers for 0.51 and $1.01 \mu\text{m}$ spheres.

surement of CR at each depth. [Theoretically, about 350 independent measurements would be necessary to obtain accurate CR measurements (to within 0.02).]

Figure 2 shows plots of the mean voltage signal and CR versus axial position corresponding to the measurements of $0.51 \mu\text{m}$ spheres. The mean curves show that the relative signal strength is strictly increasing with sphere concentration. Each CR curve shows a sharp peak at the center of the confocal gate. As the beam diverges away from its focal point, the contrast ratio rapidly decreases as large numbers of scatterers begin to contribute to the signal. (Multiple scattering effects and system sensitivity limitations are also significant in this region.) Figure 3 shows a plot of CR at the peak signal location versus ENS, for both 0.51 and $1.01 \mu\text{m}$ spheres. In both cases, the experimental results support the theoretical predictions. For ENS values of 5 or less, Fig. 3 shows a rapid increase in CR. For extreme CR values (over 1.2), interference within the sample probe volume is rare, so the OCT images do not clearly display speckle. However, the experiment shows the validity of the theory in this region; the maximum measured CR value is in excess of 2.

According to Mie theory, if $\text{ENS}=5$, then for our cases of 0.51 and $1.01 \mu\text{m}$ microspheres, the scatter-

ing coefficient is 3.7 and 78 cm^{-1} , respectively. If one reduces the refractive index contrast to 1.06 , a value more typical of tissue,¹² and considers sphere sizes ranging from 1 to $3 \mu\text{m}$ (corresponding to volume fractions from 0.01 to 0.2), then the same calculation yields scattering coefficients ranging from 10 to 500 cm^{-1} . This range includes many typical scattering coefficients reported for various tissue types,¹⁴ suggesting that speckle contrast ratio is a potentially feasible means of discriminating between different sample regions. Other factors, including the continuum of scatterer sizes, must be taken into account before the broad applicability of this technique to tissue is confirmed. Its effectiveness would be increased if higher bandwidth sources and/or higher-resolution objective lenses were utilized to decrease the sample probe volume.

We have demonstrated that the speckle contrast ratio is correlated with the concentration of scatterers in the OCT sample probe volume, and have shown good agreement between experimental results and the predictions of a theoretical random phasor sum model. A simple Mie-theoretical analysis suggests that, particularly in ultrahigh-resolution regimes, OCT speckle contrast ratio could be used to distinguish sample regions with different microscopic properties. That is, under appropriate conditions, static speckle statistics could be used as an information source in OCT.

T. R. Hillman's e-mail address is hillm-tr@ee.uwa.edu.au.

References

1. D. Huang, E. A. Swanson, C. P. Lin, J. S. Schuman, W. G. Stinson, W. Chang, M. R. Hee, T. Flotte, K. Gregory, C. A. Puliafito, and J. G. Fujimoto, *Science* **254**, 1178 (1991).
2. J. M. Schmitt, S. H. Xiang, and K. M. Yung, *J. Biomed. Opt.* **4**, 95 (1999).
3. J. C. Dainty, ed. *Laser Speckle and Related Phenomena*, 2nd ed. (Springer, 1984).
4. Y. Pan, R. Birngruber, J. Rosperich, and R. Engelhardt, *Appl. Opt.* **34**, 6564 (1995).
5. D. D. Sampson and T. R. Hillman, in *Lasers and Current Optical Techniques in Biology*, G. Palumbo and R. Pratesi, eds. (Royal Society of Chemistry, 2004).
6. M. Pircher, E. Götzinger, R. Leitgeb, A. F. Fercher, and C. K. Hitzenberger, *J. Biomed. Opt.* **8**, 565 (2003).
7. D. A. Boas, K. K. Bizheva, and A. M. Siegel, *Opt. Lett.* **23**, 319 (1998).
8. Y. Imai and K. Tanaka, *J. Opt. Soc. Am. A* **16**, 2007 (1999).
9. Y. Zhao, Z. Chen, C. Saxer, Q. Shen, S. Xiang, J. F. de Boer, and J. S. Nelson, *Opt. Lett.* **25**, 114 (2000).
10. K. W. Gossage, T. S. Tkaczyk, J. J. Rodriguez, and J. K. Barton, *J. Biomed. Opt.* **8**, 570 (2003).
11. J. W. Goodman, *Statistical Optics* (Wiley-Interscience, 1985).
12. J. M. Schmitt and G. Kumar, *Appl. Opt.* **37**, 2788 (1998).
13. A. Abdi, H. Hashemi, and S. Nader-Esfahani, *IEEE Trans. Commun.* **48**, 7 (2000).
14. V. Tuchin, *Tissue Optics* (SPIE, 2000).